

Suppression of electron–electron repulsion and superconductivity in ultra-small carbon nanotubes

This article has been downloaded from IOPscience. Please scroll down to see the full text article.

2006 J. Phys.: Condens. Matter 18 S2115

(<http://iopscience.iop.org/0953-8984/18/33/S27>)

View [the table of contents for this issue](#), or go to the [journal homepage](#) for more

Download details:

IP Address: 129.252.86.83

The article was downloaded on 28/05/2010 at 13:02

Please note that [terms and conditions apply](#).

Suppression of electron–electron repulsion and superconductivity in ultra-small carbon nanotubes

S Bellucci¹, M Cini^{1,2}, P Onorato¹ and E Perfetto^{1,3}

¹ INFN, Laboratori Nazionali di Frascati, PO Box 13, 00044 Frascati, Italy

² Dipartimento di Scienze Fisiche, Università di Roma Tor Vergata, Via della Ricerca Scientifica, Roma, Italy

³ Instituto de Estructura de la Materia, Consejo Superior de Investigaciones Científicas, Serrano 123, 28006 Madrid, Spain

Received 13 January 2006

Published 4 August 2006

Online at stacks.iop.org/JPhysCM/18/S2115

Abstract

Recently, ultra-small diameter single wall nanotubes with diameter of ~ 0.4 nm have been produced and many unusual properties were observed, such as superconductivity, leading to a transition temperature $T_c \sim 15$ K, much larger than that observed in the bundles of larger diameter tubes.

By a comparison between two different approaches, we discuss the issue of whether a superconducting behaviour in these carbon nanotubes can arise by a purely electronic mechanism in the armchair geometry. The first approach is based on the Luttinger model while the second one, which emphasizes the role of the lattice and short range interaction, is developed starting from the Hubbard Hamiltonian. By using the latter model we predict a transition temperature of the same order of magnitude as the measured one.

(Some figures in this article are in colour only in the electronic version)

1. Introduction

Carbon nanotubes (CNs) are basically rolled up sheets of graphite (hexagonal networks of carbon atoms) forming tubes that are only nanometres in diameter and have length up to some microns. Several experiments in the last 15 years have shown their interesting properties [1]. The nanometric size of CNs, together with the unique electronic structure of a graphene sheet, make the electronic properties of these one-dimensional (1D) structures highly unusual. In fact, the electronic properties of CNs depend on their diameter and chiral angle (helicity) parametrized by a roll-up (wrapping) vector (n, m) [2]. Hence it follows that some nanotubes are metallic with high electrical conductivity, while others are semiconducting with relatively low bandgaps. CNs may also display different behaviours depending on whether they are single walled carbon nanotubes (SWNTs; an individual SWNT has typical dimensions $L \sim 1 \mu\text{m}$ and $R \sim 1$ nm) or multi-walled carbon nanotubes (MWNTs) that are typically made of several

(typically 10) concentrically arranged graphene sheets with a radius of about 5 nm and lengths in the range of 1–100 μm .

In the following we will study the possibility that a superconducting behaviour can arise, at least in a special class of CNs, by a purely electronic mechanism, i.e. neglecting the contribution of phonons, but rather concentrating on the effect of rescaling the e–e repulsion for obtaining superconductivity. Hence, we first review the concept of a Luttinger liquid, in particular for CNs, with the corresponding interaction range and transport behaviour, before describing superconducting correlations in CNs.

1.1. The concept of a Luttinger liquid

Electronic correlations have been predicted to dominate the characteristic features in quasi-one-dimensional (1D) interacting electron systems. These properties, commonly referred to as Tomonaga–Luttinger liquid (TLL) behaviour [3], are very different from those of a Fermi liquid, because Landau quasiparticles are unstable and the low energy excitation is achieved by exciting an infinite number of plasmons (collective electron–hole pair modes), making the transport intrinsically different. Thus, the electron–electron (e–e) interaction modifies significantly the transport properties (the conductance G) also of CNs and leads to the formation of a Luttinger liquid (LL) with properties very different from those of the non-interacting Fermi gas [3, 4].

1.2. Luttinger liquid behaviour in carbon nanotubes

The LL behaviour implies the power-law dependence of physical quantities, such as for the tunnelling density of states (DOS), as a function of the energy or the temperature. The tunnelling conductance G reflects the power law dependence of the DOS in a small bias experiment [5]

$$G = dI/dV \propto T^{\alpha_{\text{bulk}}} \quad (1)$$

for $eV_b \ll k_B T$, where V_b is the bias voltage, T is the temperature and k_B is Boltzmann's constant. The bulk critical exponent can be obtained in several different ways and has the form

$$\alpha_{\text{bulk}} = \frac{1}{4} \left(g + \frac{1}{g} - 2 \right). \quad (2)$$

In previous papers [6–8], where we developed a renormalization group (RG) method in order to study the low energy behaviour of the unscreened e–e interaction in CNs, we obtained

$$\sqrt{1 + \frac{U_0(q_c)}{(2\pi v_F)}} = \frac{1}{g}, \quad (3)$$

where v_F is the Fermi velocity, $U_0(p)$ corresponds to the Fourier transform of the 1D e–e interaction potential, and $q_c = 2\pi/L$ can be assumed as the natural infrared cut-off, depending on the longitudinal length L of the quasi-1D device. Thus, g is a function of the interaction strength and $g < 1$ corresponds to a repulsive interaction. Thus evidence of LL behaviour has been found in many experiments [9–11] in SWNT [11], where a measurement of the temperature dependence of the resistance was carried out, above a crossover temperature T_c [12].

1.3. Range of the interaction and transport

The crucial role played by the range of the interaction in CNs, in order to explain the LL behaviour of large multi-wall [6] and doped [7, 8] CNs, was also analysed by using RG methods. Nevertheless, at $T \lesssim 1$ K the conductance, G , of an SWNT showed typical Coulomb blockade (CB) peaks in the zero bias G and allowed us to investigate the energy levels of interacting electrons. In this case, crudely described by the CB mechanism [13], periodic peaks (Coulomb oscillations) are observed in the conductance as a function of the gate potential [14, 15].

The effects of a long range interaction have to be observed also in the transport at very low temperature as we discuss below. In a recent paper [16] we investigated the effects of the long range terms of the interaction in an SWNT and compared our results with recent experiments at very low temperature T [17]. In that paper we explained the observed damping in the addition energy for SWNTs [17] at $T \sim 200$ mK as an effect of the long range of the e–e repulsion.

1.4. Superconductivity

Experiments have been also carried out to probe superconducting (SC) correlations in CNs. Clear evidence of SC correlations was found in a CN attached to suitable contacts [18, 19]. Supercurrents have been observed in the samples with SC electrodes reported in [18], providing evidence of the proximity effect in the CN. Moreover, SC transitions have been measured in nanotube ropes attached to highly transparent contacts [20].

Recently, ultra-small diameter SWNTs (diameter ~ 0.4 nm) have been produced inside zeolite channels (with inner diameter of ~ 0.73 nm). The ultra-small diameter of these tubes gives them many unusual properties, such as superconductivity, leading to a transition temperature $T_c \approx 15$ K [21], much larger than that observed in bundles of larger diameter tubes [22].

1.5. The small diameter SC CN

In [21] the nanotube diameter $d = 4.2 \pm 0.2$ Å is closer to the value calculated for a (3, 3) CN geometry, although the presence of (5, 0) nanotubes cannot be discarded [23]. Next we refer to these ultra-small nanotubes as US CNs. It has been shown by using the local-density functional method that the (3, 3) nanotubes have the same band structure of typical armchair nanotubes near the Fermi level, with a pair of subbands crossing at two opposite momenta [23]. In order to observe the supercurrents, it is necessary to fabricate thin samples to ensure that there is no potential barrier within the length of the SWNTs. This is done by further reducing the length of the CNs to about 50–100 nm, thus we assume, in the following, the length of the US CNs to be $L \sim 50$ nm.

1.6. Electron–phonon assisted superconductivity

These experiments have stimulated a significant amount of work at the theoretical level, in order to understand the origin of the superconducting transition [24–27], where the electron–phonon interaction plays a crucial role in the standard superconductivity. In a recent paper [28], the authors verify that the electron–phonon coupling parameter in the armchair geometry originates mainly from phonons at $q = 2k_F$ and is strongly enhanced when the diameter decreases.

1.7. Summary

In this paper we want to discuss whether a superconducting behaviour can arise, at least in US CNs, by a purely electronic mechanism, i.e. from purely repulsive e–e interactions. Thus, we do not include phonons in our model even if we acknowledge that their contribution could be relevant. Here we focus on armchair nanotubes, although the presence of zig-zag (5, 0) metallic nanotubes in the zeolite matrix cannot be discarded.

In order to pursue our aim we investigate the effective range of the e–e interaction because the rescaling of the e–e repulsion is crucial for obtaining superconductivity. In fact, if we start from the analysis of the LL theory for an SWNT developed in [4], we find that a purely electronic mechanism which gives superconductivity needs the screening of the forward scattering (long range effect), the increasing of the backward scattering (short range effect) and relevant effects from the lattice (very short range effects).

When the short range component of the electron–electron interaction and the effects of the lattice cannot be neglected, the usual approach to the Luttinger model breaks down. Therefore, we have to introduce a model which better describes the very short range term of the interaction, as well as the localization of the electrons on the lattice, as is the case of the Hubbard Hamiltonian.

2. Luttinger liquid approach

In order to analyse the effects due to the size of the CNs on their properties we first discuss the behaviour of SWNTs with a radius rather larger than that of the US CNs.

The LL theory for an SWNT was developed in [4] where the low energy theory including Coulomb interactions is derived and analysed. It describes two fermion chains without interchain hopping but coupled in a specific way by the interaction. The strong-coupling properties are studied by bosonization, and consequences for experiments on single armchair nanotubes are discussed. The remarkable electronic properties of carbon nanotubes are due to the special band structure of the π electrons in graphite [29, 30]. The discussion in this paper is limited to transport through metallic armchair (n, n) SWNTs; in particular, we discuss the case of the (10, 10) CN with a length $L = 3 \mu\text{m}$ and we name it CN₁₀. Thus we have the characteristic dispersion relation of a metallic SWNT which exhibits two distinct Fermi points at $\vec{K} = (\pm 4\pi/3a, 0)$ and $\alpha = \pm$ with a right- and a left-moving ($r = R/L = \pm$) branch around each Fermi point. These branches are highly linear with Fermi velocity $v_F \approx 8 \times 10^5 \text{ m s}^{-1}$. The R- and L-movers arise as linear combinations of the $p = \pm$ sublattice states reflecting the two C atoms in the basis of the honeycomb lattice. The dispersion relation holds for energy scales $E < D$, with the bandwidth cut-off scale $D \approx \hbar v_F/R$ for tube radius R . We choose the y -axis points along the tube direction and the circumferential variable is $0 \leq x \leq 2\pi R$, where $R = \sqrt{3}na/2\pi$ is the tube radius. The lattice constant is $a = 2.46 \text{ \AA}$.

As concerns the interaction we distinguish three processes associated with the Fermi points $\pm K_s$. First, we have ‘forward scattering’ (g_2 with small transferred momentum i.e. $p \sim q_c$). Second, we have ‘backscattering’ (g_1 with large transferred momentum i.e. $p \sim 2K_s$). Finally, at half-filling there is an additional ‘Umklapp’ process that in our case we neglect, since the sample is assumed to be doped.

An additional ‘Forward scattering’ term (f) which measures the difference between intra- and inter-sublattice interactions, can be introduced following [4]. This term is due to the hard core of the Coulomb interaction, i.e. it follows from the unscreened short range component of the interaction.

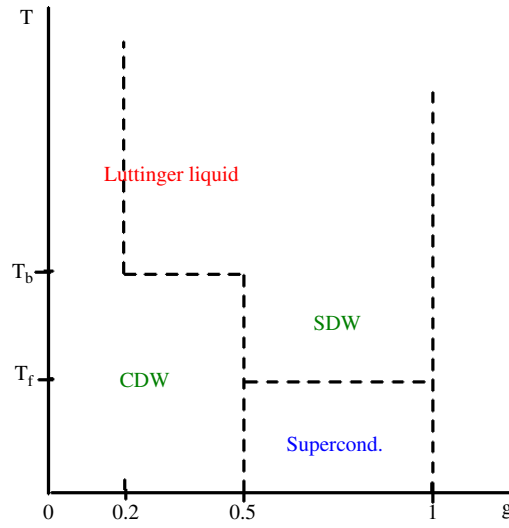


Figure 1. Effective field theory was solved in a practically exact way by Egger and Gogolin [4]. They concluded that low temperature phases matter only for ultrathin tubes or in the sub-millikelvin regime. The temperature T_b depends on the strength of the backward scattering term (g_1), T_f depends on the relevance of the lattice effects while g depends on the forward scattering (usually g_2).

2.1. Electron–electron interaction

Now, by following Egger and Gogolin [4], we introduce the unscreened Coulomb interaction in two dimensions

$$U_0(\mathbf{r} - \mathbf{r}') = c_0 \frac{e^2}{\sqrt{(x - x')^2 + 4R^2 \sin^2\left(\frac{\varphi - \varphi'}{2}\right)}}. \quad (4)$$

Then, we can calculate $U_0(q)$ as

$$U_0(q) \approx \frac{c_0 e^2}{\sqrt{2}} \left[K_0\left(\frac{qR}{2}\right) I_0\left(\frac{qR}{2}\right) \right], \quad (5)$$

where $K_0(q)$ denotes the modified Bessel function of the second kind, $I_0(q)$ is the modified Bessel function of the first kind and R , the CN's radius, acts as a natural cut-off of the interaction. It is clear that the interaction in equation (5) does not contain the effects at very short range due to the additional forward scattering (f coupling).

2.2. The phase diagram

Effective field theory was solved in a practically exact way by Egger and Gogolin [4]. They obtained for the CN₁₀ a value of $g \approx 0.2$ corresponding to $\alpha_{\text{bulk}} \approx 0.32$ in agreement with experiments. They also predict the presence of an SC phase due to the effect of g_1 and f , but at very low temperatures ($T_b \sim 0.1$ mK and $T_f \lesssim T_b$; see figure 1).

Starting from these results a pure electronic mechanism which gives superconductivity needs the following:

- (i) screening of the forward scattering, g_2 (long range effect $g > 0.5$);
- (ii) increasing of the backward scattering, g_1 (short range effect T_b);
- (iii) relevant effects from the lattice (high value of the corresponding temperature, T_f).

Calculations for a CN_{10} predict that 1D superconductivity is the dominant instability only at $T < 1$ mK with screened interactions, thus a purely electronic mechanism is not sufficient. Can this effect be relevant in US CNs?

3. Effects of the screening

Now we want to discuss some screening effects that can be relevant in CNs by focusing on the role played by the size and on the reduction of the effective range of the interaction.

3.1. Intratube screening

One electron screening effect can be taken into account by analysing how the interaction dresses the bare electron propagator with the polarization. The one loop polarizability $\Pi_0(k, \omega_k)$ is given by the sum of particle-hole contributions within each branch

$$\Pi_0(k, \omega_k) = \frac{1}{h} \frac{v_F k^2}{|v_F^2 k^2 - \omega_k^2|}. \quad (6)$$

The effective interaction is found by the Dyson equation:

$$U_{\text{eff}}(k, \omega_k) = \frac{U_0(k)}{1 + U_0(k)\Pi_0(k, \omega_k)}. \quad (7)$$

This approximation is well justified in 1D as long as we focus on the long range part of the interaction ($k \sim q_c$) [31]. Thus the random phase approximation (RPA) for the dielectric function follows from the previous formula as

$$\kappa(q, \omega_q) = 1 + U_0(q)\Pi_0(q, \omega_q).$$

In order to investigate the size dependent dielectric function we can introduce the bandwidth cut-off scale $D = v_F \hbar / R$ as the scale for the UV cut-off energy. Thus we introduce the dimensionless frequency $\nu = \omega / (v_F q)$ which ranges from $-1/(qR)$ to $1/(qR)$ and we obtain

$$\kappa(q) = 1 + \int_{-1/(qR)}^{1/(qR)} d\nu (U_0(q)\Pi_0(q, \nu)) \approx 1 + \frac{U_0(q)}{2\pi \hbar v_F} \left| \ln \left(\left| \frac{qR + 1}{qR - 1} \right| \right) \right|.$$

Now we can evaluate the size dependent screening as $g_i \rightarrow \tilde{g}_i = g_i / \kappa$, for the different CNs corresponding to the different processes (here we name \tilde{g}_i the screened interaction). For the forward scattering we obtain a size dependent rescaling of the interaction

$$g_2 \longrightarrow \begin{cases} \tilde{g}_2 = 0.90g_2 & \text{for CN}_{10} \\ \tilde{g}_2 = 0.61g_2 & \text{for USCN.} \end{cases} \quad (8)$$

Concerning the rescaling of g_1 the RPA approximation does not give correct results. In this case we should resort to the RG technique; anyway, as shown in [4], g_1 gets modified only at very low temperatures.

3.2. Screening by the contacts

Another source of the electron screening comes from the presence of the contacts, and it can be analysed by the introduction of two charge images.

As we show in figure 2 this kind of screening gives a strong suppression of the long range component of the interaction (a constant interaction with infinite range is totally erased) while the short range one is almost unaffected. A size dependent screening of the interaction, greater

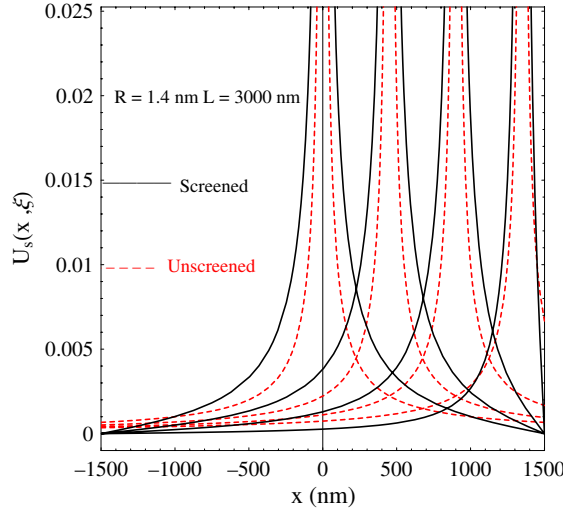


Figure 2. In this figure the e–e repulsion is shown as a function of the electron position in a CN₁₀. One charge is put at the centre of the CN or at 450, 900 and 1350 nm from the centre. The screening due to the contacts gives a strong suppression of the long range component of the interaction (a constant interaction with infinite range is totally erased) while the short range one is almost unaffected (increased).

in the US CN than in the usual CN₁₀, follows for the forward scattering. We estimate that the long range interaction in the US CN is reduced by about 7% more than in the CN₁₀, i.e.

$$\tilde{g}_2^{\text{USCN}} \approx 0.93 \frac{\tilde{g}_2^{\text{CN}_{10}}}{g_2^{\text{CN}_{10}}} g_2^{\text{USCN}}.$$

3.3. Screening by the zeolite matrix

A further important source of screening arises from the other nanotubes in the surrounding zeolite matrix. As already pointed out in [32], the intra-tube Coulomb repulsion at small momentum transfer (i.e. in the forward scattering channel) is efficiently screened by the presence of electronic currents in neighbour nanotubes. In the experimental samples of [21] the carbon nanotubes are arranged in large arrays with triangular geometry, behaving as a genuine 3D system. By means of a generalized random phase approximation approach, it is shown [32] that the forward scattering parameter g_2 is renormalized according to the Dyson equation

$$g_2 \rightarrow \frac{1}{2\pi v_F} \left(\frac{d}{2\pi} \right)^2 \int_{\text{BZ}} d^2\mathbf{p} \frac{\phi(k \approx 0, \mathbf{p})}{1 - \Pi(k \approx 0)\phi(k \approx 0, \mathbf{p})}, \quad (9)$$

where $d \approx 1$ nm is the intertube distance in the matrix whose Brillouin zone is denoted by BZ, $\Pi(k) = \frac{2}{L} \sum_q \frac{f(\epsilon_{q+k}) - f(\epsilon_q)}{\epsilon_{q+k} - \epsilon_q}$, and $\phi(k, \mathbf{p})$ is the Fourier transform of the 3D Coulomb potential with longitudinal momentum k and 2D transverse momentum \mathbf{p} . The above source of screening provides a large reduction of g_2 (by a factor of $\approx 10^{-2}$), while the backscattering coupling g_1 is not affected appreciably [32].

We conclude this analysis by pointing out that in the superconducting samples of [21] the long range part of the Coulomb repulsion can be reduced by a total factor of the order of $\lambda \approx 10^{-3}$, while the short range one is essentially unmodified, at least in the temperature range of the experimental conditions.

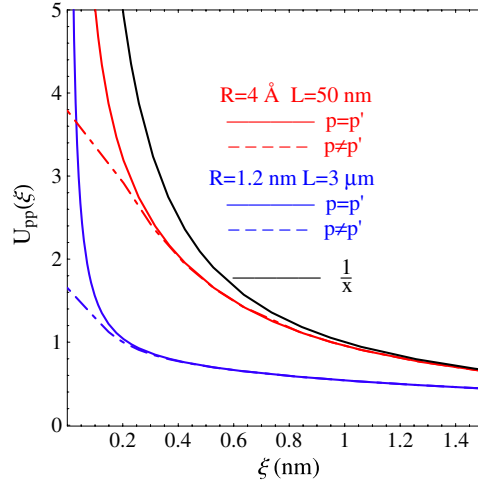


Figure 3. The e-e repulsion. The interaction between electrons belonging to different sublattices $p \neq p'$ has a short range component rather smaller than the interaction between electrons belonging to the same sublattice $p = p'$.

3.4. Unscreened parameters: the short range component

As we discussed above, the short range interaction contributes to two fundamental parameters. The first one, the backward scattering term, has to be stronger in small diameter CNs; in fact we calculate $g_1 \sim 0.067(2\pi v_F)$ in CN_{10} ($g_1/g_2 \sim 0.003$) and $g_1 \sim 0.45(2\pi v_F)$ in US CN ($g_1/g_2 \sim 0.04$), thus $g_1^{\text{US}} \sim 6.5g_1^{\text{CN}_{10}}$.

The temperature T_b reported in the phase diagram of figure 1 was calculated in [4] as

$$kT_B \propto D \exp\left(\frac{2\pi v_F}{g_1}\right),$$

and was estimated for the CN_{10} in the order of $T_b \sim 0.1$ mK. It follows that in US CNs T_b should be several orders of magnitude larger than the one predicted for a CN_{10} with a factor compatible with the observed critical temperature.

The coupling constant $f > 0$, even though it can be assumed as a forward scattering term, strongly depends on the nanotube geometry and the short range component of the interaction. In fact when we consider two interacting electrons at a very short distance, the fact of belonging to the same sublattice, or not, becomes relevant as we show in figure 3. In order to calculate f on the wrapped graphite lattice, we can start from the microscopic arrangement of carbon atoms around the waist of the armchair SWNT. Following [4] is quite easy to demonstrate that $f \propto \frac{1}{n}$ for an (n, n) CN, so we obtain that it is 10/3 times larger in the US CN than in the CN_{10} .

3.5. Breakdown of the Luttinger approach

Now we analyse the additional forward scattering f . It corresponds to [4] $\delta V_p = U_{++} - U_{+-}$, where $U_{p,p'}$ is the interaction between electrons belonging to different sublattices (p, p'). In figure 3 we plot $U_{p,p'}$ both for the CN_{10} and US CN. We observe that, because of the rapidly oscillating phase factor, the only non-vanishing contribution to g_1 comes from $|x - x'| \leq a$ [4]. Therefore, we can conclude that a local interaction is relevant in CNs. This very short range interaction is strongly suppressed at a distance much larger than $\ell \sim 0.3$ nm, enforcing the

validity of a short range model (like the Hubbard one) for the small radius CN where this contribution, f , is comparable to g_2 . We suppose that the LL theory, which just predicts a charge density wave instability for $g \lesssim 0.5$, could not include the strong effects of the lattice and short range component of the interaction which could be dominant in US CNs. In fact, because of the dominance of the short range component of the electron–electron interaction, the effects of the lattice in the US CN cannot be neglected or treated as a perturbation.

Thus we suggest the presence of an SC phase, where the lattice effects and the very short range interaction become dominant. In our opinion this kind of system should be better described in the Hubbard-like approach than by using the LL theory.

4. Hubbard model

The possibility of a superconducting phase in CNs in the framework of the Hubbard model has been discussed in some papers in the past [33, 34].

Krotov and coworkers [34] used an on-site (U) and nearest-neighbour interaction (V) to model the screened e–e repulsion. It follows, for slightly doped samples, that a superconducting phase is present for values of parameters $\frac{V}{U} < 0.55$, signalling that the pure Hubbard model ($V = 0$) would show superconductivity. Our previous discussions about the screening of the interaction and the corresponding reduction of its range confirm that the superconductivity phase is supported by the size of the US CN. Unfortunately, the approach of [34] does not allow the estimation of the critical temperature T_c .

In [33, 35] the authors explored an electronic mechanism which *per se* leads to bound pairs starting from the pure Hubbard model. The notion that pairing can arise by a purely electronic mechanism, i.e. from purely repulsive e–e interactions, was put forth by Kohn and Luttinger long ago [36]. They suggested that for large odd values of the relative angular momentum two electrons could stay far enough apart from each other to take advantage of the Friedel oscillations of the screened Coulomb potential. In the approach based on a 2D Hubbard model the first-order Coulomb repulsion is removed by symmetry.

In [33] it was shown that the Hubbard Hamiltonian for a CN admits two-body singlet eigenstates with no double occupancy, called $W = 0$ pairs. The electrons forming a $W = 0$ pair have no direct interaction and are the main candidates to achieve bound states in purely repulsive Hubbard models already used for the cuprates [35].

Following the approach developed in [33] we can evaluate the superconducting gap, Δ , which is strongly dependent on the size of the CN. In fact, as discussed in [4] and references therein [34, 37], in the language of the Hubbard-like models we have $f \propto U$, thus the on-site Coulomb interaction U can be assumed to be proportional to $1/n$. Thus the energy gap Δ can be estimated to be about 3 orders of magnitude greater in the US CN than in the CN_{10} . In the US CN away from half-filling we can evaluate the values of Δ . The BCS theory estimates the zero-temperature energy gap

$$\Delta(0) \approx 1.76k_B T_c,$$

thus for a US CN we are able to estimate the crossover temperature

$$T_c \approx 5\text{--}50 \text{ K}$$

of the same order as the measured one while the corresponding T_c for the CN_{10} is of the order of the m^{-K} in agreement with the discussed predictions of [4].

Now we want to discuss the consistency of the above results by using two different criteria. In order to do this it is useful to estimate the coherence length ξ_c of the Cooper pairs in US CNs,

which can be obtained by the well known relation

$$\xi_c = \frac{\hbar v_F}{\pi \Delta(0)}.$$

We estimate ξ_c of some tens of nanometres, which is of the same order as the CN's length.

The first criterion in order to establish the validity of the Hubbard model concerns the value of the interaction at distance $r \sim \xi_c$, which has to be many times smaller than the energy gap Δ ,

$$\frac{\lambda e^2}{\xi_c} \ll \Delta(0).$$

In our case this condition is verified ($\lambda \sim 10^{-3}$) because of the strong screening, especially due to the zeolite matrix.

The second criterion in order to ensure that the electrons forming the Cooper pairs feel a short range interaction is based on the comparison between ξ_c and the characteristic range of the screened interaction ℓ (see figure 3),

$$\xi_c \gg \ell.$$

Also this condition is fairly well fulfilled and confirms the consistency of the approach based on the Hubbard model.

5. Conclusion

The discovery of superconductivity at 15 K in SWNTs challenges the usual phonon mechanism of superconductivity no less than the similar discovery of superconductivity [38] at 6.5° in C₆Yb and at 11.5° in C₆Ca intercalated graphite. In both cases the possibility that the electrons themselves provide the driving force must be taken into account. This means that it should be possible in some fashion to go all the way from the e–e repulsion to an effective attraction and to bound pairs. This is a time-honoured dream that potentially has conceptual appeal as well as important practical implications, but a convincing mechanism must predict which properties of the material are important to produce superconductivity. For instance, one could consider replacing phonons by plasmons in the usual mechanism; the weakness of such an approach is that plasmons exist in any material, and have comparable frequencies, so everything should superconduct at several kelvin. The $W = 0$ mechanism is based on the point symmetry of the lattice and predicts pairing in cuprates and in graphite-based materials on the same grounds. Unlike the original suggestion by Kohn and Luttinger [36], which has not yet been borne out by experiments, SWNTs (*in vacuo* or in a matrix) and intercalated graphite are anisotropic inhomogeneous systems. They are so different that the respective mechanisms can differ in important ways, yet they have the honeycomb lattice in common, i.e. the local symmetry is the same and leads to $W = 0$ pairs. The hexagonal lattice leads to pairing in a Hubbard model, but the long range part of the repulsion must be disposed of if we want the on-site repulsion to operate undisturbed, and here nanotubes and graphite obviously pose quite different problems; the SWNT is the harder case to understand, since screening works better in 3D than in 1D. In this paper we have focused on this problem and provided possible explanations based on the residual screening effects augmented by a powerful matrix and contact contribution. Furthermore, we pointed out that the range of the interaction must be small compared to the pair size, but it should not necessarily be cut down to a lattice parameter. Although this proposal clearly needs further scrutiny before being validated, we feel it is serious enough to warrant further investigation.

References

- [1] Ebbesen T W 1996 *Phys. Today* **49** (6) 26
Smalley R E 1997 *Rev. Mod. Phys.* **69** 723
Collins P G, Zettl A, Bando H, Thess A and Smalley R E 1997 *Science* **278** 100
- [2] Mintmire J W, Dunlap B I and White C T 1992 *Phys. Rev. Lett.* **68** 631
Hamada N, Sawada S and Oshiyama A 1992 *Phys. Rev. Lett.* **68** 1579
Saito R, Fujita M, Dresselhaus G and Dresselhaus M S 1992 *Appl. Phys. Lett.* **60** 2204
- [3] Tomonaga S 1950 *Prog. Theor. Phys.* **5** 544
Luttinger J M 1963 *J. Math. Phys.* **4** 1154
Mattis D C and Lieb E H 1965 *J. Math. Phys.* **6** 304
- [4] Egger R and Gogolin A O 1997 *Phys. Rev. Lett.* **79** 5082
Egger R and Gogolin A O 1998 *Eur. Phys. J. B* **3** 281
- [5] Kane C L and Fisher M P A 1992 *Phys. Rev. B* **46** 15233
Kane C L and Fisher M P A 1992 *Phys. Rev. Lett.* **68** 1220
- [6] Bellucci S and González J 2000 *Eur. Phys. J. B* **18** 3
Bellucci S 1999 *Path Integrals from peV to TeV* ed R Casalbuoni *et al* (Singapore: World Scientific) p 363
(Preprint [hep-th/9810181](#))
Bellucci S and González J 2001 *Phys. Rev. B* **64** 201106(R)
- [7] Bellucci S, González J and Onorato P 2003 *Nucl. Phys. B* **663** 605 [FS]
Bellucci S and Onorato P 2006 *Ann. Phys.* **321** 934
(Bellucci S and Onorato P 2005 Preprint [cond-mat/0510590](#))
- [8] Bellucci S, González J and Onorato P 2004 *Phys. Rev. B* **69** 085404
Bellucci S, González J and Onorato P 2005 *Phys. Rev. Lett.* **95** 186403
Bellucci S, González J, Onorato P and Perfetto E 2006 *Phys. Rev. B* submitted
(Bellucci S, González J, Onorato P and Perfetto E 2005 Preprint [cond-mat/0512546](#))
- [9] Yao Z, Postma H W, Balents L and Dekker C 1999 *Nature* **402** 273
- [10] Kane C, Balents L and Fisher M P A 1997 *Phys. Rev. Lett.* **79** 5086
- [11] Bockrath M, Cobden D H, Lu J, Rinzler A G, Smalley R E, Balents L and McEuen P L 1999 *Nature* **397** 598
- [12] Fischer J E, Dai H, Thess A, Lee R, Hanjani N M, Dehaas D L and Smalley R E 1997 *Phys. Rev. B* **55** R4921
- [13] Beenakker C W J 1991 *Phys. Rev. B* **44** 1646
- [14] Bockrath M, Cobden D H, McEuen P L, Chopra N G, Zettl A, Thess A and Smalley R E 1997 *Science* **275** 1922
- [15] Tans S J, Devoret M H, Groeneveld R J A and Dekker C 1997 *Nature* **386** 474
- [16] Bellucci S and Onorato P 2005 *Phys. Rev. B* **71** 075418
- [17] Cobden D H and Nygard J 2002 *Phys. Rev. Lett.* **89** 46803
- [18] Kasumov A Yu *et al* 1999 *Science* **284** 1508
- [19] Morpurgo A F *et al* 1999 *Science* **286** 263
- [20] Kociak M *et al* 2001 *Phys. Rev. Lett.* **86** 2416
Kasumov A *et al* 2003 *Phys. Rev. B* **68** 214521
- [21] Tang Z, Zhang L, Wang N, Zhang X, Wen G, Li G, Wang J, Chan C and Sheng P 2001 *Science* **292** 2462
- [22] Kociak M, Kasumov A Y, Gueron S, Reulet B, Khodos I I, Gorbatov Y B, Volkov V T, Vaccarini L and Bouchiat H 2001 *Phys. Rev. Lett.* **86** 2416
- [23] Liu H J and Chan C T 2002 *Phys. Rev. B* **66** 115416
- [24] Gonzalez J 2001 *Phys. Rev. Lett.* **87** 136401
- [25] González J 2001 *Phys. Rev. B* **87** 136401
González J 2002 *Phys. Rev. Lett.* **88** 076403
Alvarez J V and González J 2003 *Phys. Rev. Lett.* **91** 076401
- [26] Sedeki A, Caron L G and Bourbonnais C 2002 *Phys. Rev. B* **65** 140515(R)
- [27] Kamide K, Kimura T, Nishida M and Kuhihara S 2003 *Phys. Rev. B* **68** 024506
Kamide K, Kimura T, Nishida M and Kuhihara S 2004 *Phys. Rev. B* **70** 212504
- [28] Connetable D, Rignanese G M, Charlier J C and Blase X 2005 Preprint [cond-mat/0501113](#)
- [29] Wallace P R 1947 *Phys. Rev.* **71** 622
- [30] DiVincenzo D P and Mele E J 1984 *Phys. Rev. B* **29** 1685
- [31] Solyom J 1979 *Adv. Phys.* **28** 201
- [32] González J and Perfetto E 2005 *Phys. Rev. B* **72** 205406
González J and Perfetto E 2005 Preprint [cond-mat/0510586](#)
- [33] Perfetto E, Stefanucci G and Cini M 2002 *Phys. Rev. B* **66** 165434
- [34] Krotov Y A, Lee D H and Louie S G 1997 *Phys. Rev. Lett.* **78** 4245

-
- [35] Cini M and Balzarotti A 1997 *Phys. Rev. B* **56** 14711
Cini M, Stefanucci G and Balzarotti A 1999 *Eur. Phys. J. B* **10** 293
Cini M, Perfetto E and Stefanucci G 2001 *Eur. Phys. J. B* **20** 91
- [36] Kohn W and Luttinger J M 1965 *Phys. Rev. Lett.* **15** 524
- [37] Balents L and Fisher M P A 1997 *Phys. Rev. B* **55** R11973
Balents L and Fisher M P A 1996 *Phys. Rev. B* **53** 12133
- [38] Weller T E, Ellerby M, Saxena S S, Smith R P and Skipper N T 2005 *Nat. Phys.* **1** 39–41
Csanyi G, Littlewood P B, Nevidomskyy A H, Pickard C J and Simons B D 2005 *Preprint* [cond-mat/0503569](https://arxiv.org/abs/cond-mat/0503569)